The Importance of Thermodynamic Interactions on the Dynamics of Multicomponent Polymer Systems Revealed by Examination of the Dynamics of Copolymer/Homopolymer Blends

Sudesh Y. Kamath,[†] Michael J. Arlen,[†] William A. Hamilton,[‡] and Mark D. Dadmun*[,†,§]

Department of Chemistry, The University of Tennessee at Knoxville, Knoxville, Tennessee 37996, Condensed Matter Division, Oak Ridge National Laboratory, Oak Ridge, Tennessee 37831, and Chemical Sciences Division, Oak Ridge National Laboratory, Oak Ridge, Tennessee 37831

Received February 16, 2007; Revised Manuscript Received February 1, 2008

ABSTRACT: The effect of copolymer composition on their dynamics in a homopolymer matrix has been studied using specular neutron reflectivity (NR). We have monitored the segregation process of random copolymers, containing styrene (S) and methyl methacrylate (MMA), to the d-PS/d-PMMA interface from a polymer matrix. Four random copolymers containing 50, 54, 67, and 80% MMA were studied at 10 wt % loading in d-PMMA, where the interfacial excess, Z^*, growth scaled as $t^{1/2}$ as predicted by theory. These results are correlated to the diffusion-limited growth of a copolymer wetting layer at the d-PS/d-PMMA interface. The mutual and tracer diffusion coefficients and the effective friction coefficients for these copolymers were then determined. The results demonstrate that the copolymer composition has a significant impact on its dynamics. Copolymer dynamics are significantly faster than those for a diblock copolymer at the same composition, which indicates that the impact of the change in composition is more than that due to an increase in the MMA content in the copolymer. Analysis of the friction factor using the Lodge−McLeish model indicates that the local composition around a copolymer is richer in styrene than the model predicts. We attribute this to the fact that the model uses only chain connectivity to calculate the self-concentration and does not include contributions due to thermodynamic interactions between the two blend components. The observation that the local environment around a copolymer is richer in styrene is in agreement with our simulation results and indicates that the styrene monomers in the copolymer aggregate together to minimize contact with the PMMA matrix. These results exemplify the importance of thermodynamic interactions on the dynamics of multicomponent polymer systems, particularly miscible homopolymer/copolymer blends.

Introduction

Blending two existing polymers or polymers and inorganic fillers is a cost-effective technique to produce new lightweight materials with tailored properties, and thus, these multicomponent polymer blends and composites have generated a tremendous amount of interest in recent years. However, the dynamics of multicomponent polymer systems are complicated and are not easily predicted. The effect of the presence of one component on the dynamics of the second component is not well understood. This, in turn, has a significant impact on their processability and response to an applied stress and hence their use in devices and other applications. Recent studies on miscible polymer blends[1−3] with weak thermodynamic interactions as well as disordered multiblock copolymers[4,5] suggest that the local environment in a polymer blend has a critical impact on the dynamics of each component in the blend. However, these studies do not account for the effect of thermodynamic interactions on the local environment around a polymer and hence its dynamics. Thus, there is a need for a systematic study on the effect of thermodynamic interactions between two components on their dynamics in homogeneous multicomponent systems.

In a recent study,[6] we have demonstrated that the copolymer sequence distribution can significantly impact the dynamics and structure of 50/50 copolymers dispersed in a homopolymer matrix. Our results demonstrate that random copolymers are uniformly distributed in a homopolymer matrix and have the fastest dynamics in the blend of all linear copolymer structures. Since the copolymer composition in a random copolymer has a significant impact on its local environment, we expect copolymer composition to also have a significant impact on their dynamics in a homopolymer matrix. Moreover, our simulations on the effect of copolymer composition on their dynamics in a homopolymer melt[7] demonstrate that the repulsive interactions between unlike monomers on the copolymer have a considerable impact on their local structure and environment. This in turn impacts their dynamics in a homopolymer matrix as well. Thus, a systematic study on the effects of copolymer composition on their dynamics in a homopolymer matrix should provide a critical test for theories that attribute dynamic heterogeneity to differences in the local environment and provide insight into the impact of thermodynamic interactions on the dynamics and local structure in multicomponent systems.

The composition of a copolymer affects many of its physical properties including miscibility, interfacial strengthening, viscosity, and effective friction coefficient.[8−11] Additionally, the miscibility of a copolymer in a polymer matrix dramatically affects the rate of copolymer segregation to the interface by changing the transport mechanism.[12−17] Therefore, the time dependent growth of the copolymer wetting layer at a polymer/polymer interface is expected to vary with copolymer composition. Recent studies[18] have utilized neutron reflectivity (NR) to monitor the growth of the interfacial excess, Z^*, of alternating copolymers of styrene (S) and methyl methacrylate (MMA) to the d-PS/d-PMMA interface as a function of time. This study demonstrated that NR can be effectively utilized to monitor the dynamics of the segregation of a copolymer to a bilayer interface. These results show that, for miscible polymer blends, the growth of the interfacial excess scales as $t^{1/2}$ as predicted

* Corresponding author.
[†] The University of Tennessee at Knoxville.
[‡] Condensed Matter Division, Oak Ridge National Laboratory.
[§] Chemical Sciences Division, Oak Ridge National Laboratory.

10.1021/ma0704212 CCC: $40.75
Published on Web 04/01/2008

by Kramer and Jones for the diffusion-limited growth of a polymer wetting layer.[12,13] However, for immiscible polymer blends, the interfacial excess growth scaled as $t^{1/4}$, which was previously determined to correlate to polymer domain growth by Ostwald ripening.[14–16]

It has also been demonstrated that the miscibility of a random copolymer consisting of styrene and methyl methacrylate in PMMA is dependent on copolymer composition.[8,10] There have been several studies on the effect of copolymer sequence distribution on the miscibility of binary homopolymer/copolymer blends[19] as well as ternary systems containing two homopolymers and a copolymer.[20] These studies conclude that copolymer sequence distribution plays a significant role in the phase behavior of these systems. Recent neutron reflectivity studies[21,22] suggest that some random copolymer compositions of styrene and methyl methacrylate distribute at the homopolymer/homopolymer interface in an asymmetric manner, which could lead to a weakened interface. These results indicate that the maximum toughness of the interface between PS and PMMA occurs when the copolymer has a styrene fraction of 0.68. However, the dynamics of this segregation process were not investigated. Thus, the composition and sequence distribution of a copolymer is important in determining its interactions with homopolymers and therefore can be important in determining its dynamics in a homopolymer matrix.

The effective monomeric friction factor, ζ_{eff}, of a polymer describes the friction that a polymer segment experiences as it diffuses through a polymer matrix. In this case, the polymer segment refers to a part of the chain that acts as a unit and describes the average chain length between contour changes along the polymer chain. For homopolymers, the segments consist of identical repeating units. Therefore, for homopolymers, all segments experience similar frictional forces during the segregation process. However, for copolymers, the molecular structure of the segment depends on the copolymer composition. Thus, we expect the copolymer composition to have a significant impact on the monomeric friction factor.

Along these lines, Lodge[23] used steady flow viscosity measurements to determine the ζ_{eff} values for PS, PMMA, and diblock copolymers of varying S and MMA compositions. ζ_{eff} for pure PMMA is three orders of magnitude larger than that of pure PS. This result is attributed to the fact that MMA is a larger, doubly substituted, and more polar monomer than styrene, which sterically hinders the movement of the MMA chain segments. This fact may be correlated to the segment lengths for the PS and PMMA homopolymers that are known to be 0.67 and 0.87nm, respectively.[24,25] Results by Lodge also demonstrate that the ζ_{eff} for disordered diblock copolymers increased in a log-linear fashion with composition from the ζ_{eff} value for pure PMMA to that for pure PS. The higher ζ_{eff} value of PMMA indicates that increasing the MMA composition of P(S-*co*-MMA) increases the friction that the copolymer experiences in the reptation process. Thus, increasing the MMA composition of P(S-*ran*-MMA) should inhibit the diffusion of a P(S-*ran*-MMA) copolymer through a d-PMMA matrix.

While these studies provide a wealth of information on the effect of diblock copolymer composition on their dynamics, there have been few studies on the dynamics of copolymer/homopolymer systems. Additionally, the dynamics of the segregation of a copolymer to the interface through a homopolymer matrix is a critical factor in its ability to compatibilize a polymer blend and other applications where it acts as an interfacial modifier or surfactant. Since copolymer composition is easily manipulated and has a direct impact on its local environment, these studies are ideally suited for a systematic study on the impact of the local environment on the dynamics in multicomponent polymer systems. Since PS and PMMA have significantly different friction factors, if copolymer dynamics are proportional to the MMA content, we expect to see a dramatic change in the copolymer friction factor with increasing MMA content. Another advantage of working with this system is the presence of repulsive interaction between S and MMA monomers, which allow the introduction of thermodynamic interactions in this problem, a parameter that is often assumed to be negligible in other studies. Thus, the PS/PMMA system is an ideal choice to study the impact of MMA content, local composition, and thermodynamic interactions on the dynamics in multicomponent systems.

Table 1. Molecular Weight Characteristics of the Polymers Used in This Study

polymer	M_n	M_w	M_w/M_n	% MMA
d-PMMA	49100	51100	1.04	100
d-PS	616000	671500	1.09	0
Ran80	48000	58000	1.21	80
Ran67	61900	128000	2.07	67
Ran54	52000	65000	1.25	54
Ran50	64400	89000	1.38	50

Experimental Section

Sample Preparation. Table 1 is a list of the polymers used in this project. The polymers purchased from Polymer Source were d-PMMA and d-PS, and they were used as received. Ran67 was synthesized by free radical polymerization using AIBN as the initiator. All other random copolymers were synthesized using atom transfer radical polymerization (ATRP), where the details of their synthesis and characterization can be found in the literature.[26] In all cases, polymerization was terminated at 10% conversion to minimize compositional drift. The properties of the polymers were obtained by size exclusion chromatography using four mixed columns in series, dissolved in tetrahydrofuran, and scanned at room temperature. PS homopolymer standards were used for the molecular weight calibration. H NMR was used to verify the random architecture of the copolymers as in previous studies.[27] The composition and molecular weight properties of the random copolymers are listed in Table 1. The substrates for the bilayer systems were silicon wafers that are 5 cm in diameter. The wafers were cleaned with three alternate washings of acetone and toluene, and were then placed in an ultraviolet ozone oven to provide uniform oxide surfaces. For each sample, the bottom polymer layer consists of a blend of d-PMMA and P(S-*ran*-MMA) (90/10 wt %) which was spin-coated to form a thin film approximately 65 nm thick, which were realized by spin-casting at 2500 rpm for 30 s from 1.8 vol % toluene solutions. To complete the bilayers, d-PS films, approximately 140–150 nm thick, were spin-cast at 2500 rpm for 30 s onto clean glass slides from a 2.8 vol % toluene solution. The PS films were scored on all edges with a razor and floated onto the surface of a deionized water bath. The water was carefully drained, and the films were retrieved onto the d-PMMA/P(S-*ran*-MMA) monolayer covered substrates. The bilayer samples were then dried in a vacuum oven at 60 °C for 24 h to remove any residual toluene or water.

Neutron Reflectivity. Neutron reflectivity (NR) measurements were completed on the HB-3 reflectometer (MIRROR) at the High Flux Isotope Reactor at Oak Ridge National Laboratory. NR measurements were scanned by transversing the incident neutron beam through the Si/polymer interfaces. The incident angle of reflectance was varied with a differential momentum transfer vector, $\Delta Q_z = 0.005$ Å^{-1}. The wavelength was fixed at 2.54° with a wavelength spread, $\Delta\lambda/\lambda$, of 0.02. The scattering length density (SLD) profiles were then calculated from model fits of the measured reflectivity data with the MIRROR program. After the as-cast samples were measured, the samples were annealed at 150 °C for various time intervals and quenched to room temperature, below T_g, on a cool aluminum block to stop long-range polymer motion. Reflectivity measurements were then performed. This procedure was repeated until the reflectivity profiles ceased to change with further annealing, indicating that the segregation process had

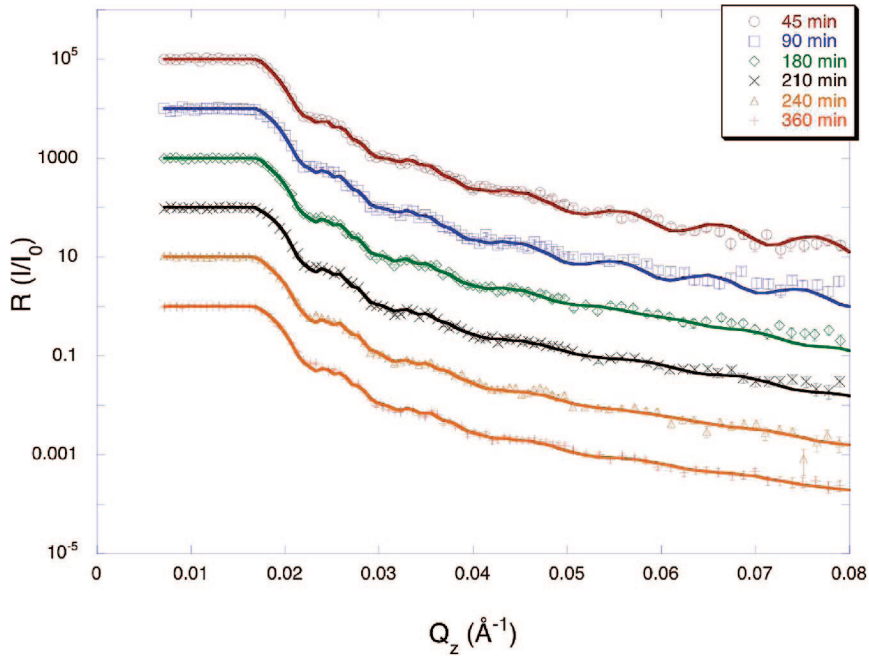

Figure 1. Evolution of the NR profiles as a function of annealing times for the ran54 bilayer sample. The symbols are the measured points, and the solid lines represent the calculated fits.

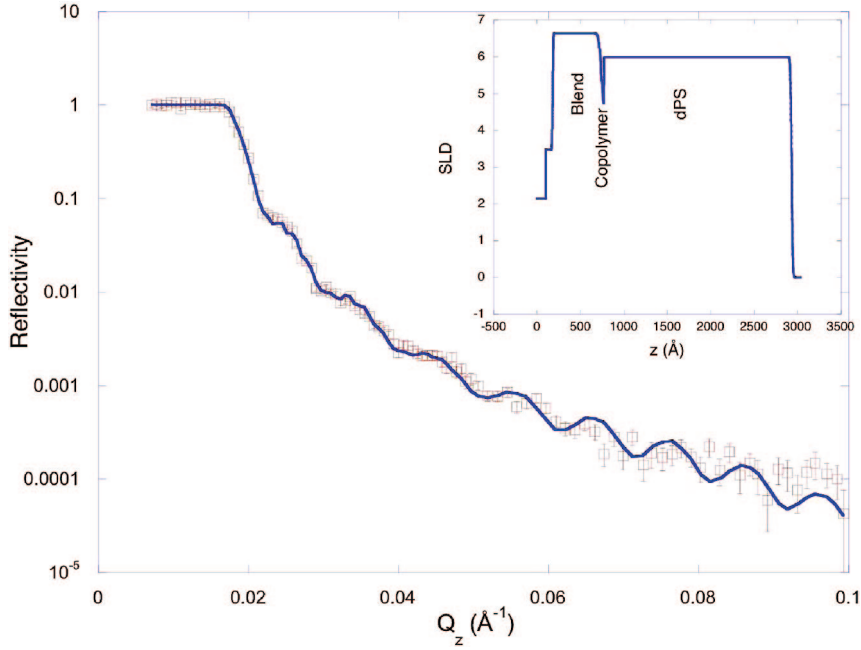

Figure 2. NR profile and fit to the ran54 bilayer sample annealed at 150 °C for 45 min. The circles are the measured points, and the solid line represents the calculated fit. The inset is the model SLD profile used to fit the reflectivity data.

reached equilibrium. Figure 1 shows the evolution of the measured reflectivity profiles as a function of annealing time for the sample with the 54% random copolymer. The best fits generated from a model SLD are also shown in the figure. Inspection of this figure documents the change in the reflectivity profile that results from the change in the interfacial structure as the copolymer segregates at the interface, most noticeably, the dampening of oscillations in the data at higher q with longer annealing time, a signature of increased interfacial roughness.

Figures 2 and 3 document these changese more clearly, where Figure 2 shows a typical reflectivity curve and fit for the bilayer sample consisting of d-PS and a 90/10 w/w d-PMMA/P(S-*ran*-MMA) blend (ran54) annealed for 45 min at 150 °C. The inset corresponds to the model SLD profile that is the best fit for the reflectivity data. Figure 3 shows the measured reflectivity profile and calculated fit for the same sample annealed for 420 min at 150 °C. A comparison of the two measured reflectivity profiles and corresponding scattering length density profiles indicates the formation of a third layer rich in hydrogenated copolymer with increasing annealing time. An expanded discussion of the differences in these two figures can be found in the Supporting Information. Examination of the model SLD profiles depicted in Figures 2 and 3 illustrates the formation of the third protonated layer, which results from the segregation of the copolymer to the interface. Thus, in a similar manner, changes in the model SLD profiles were used to monitor the growth of the interfacial region as a function of the annealing time for all copolymers listed in Table 1.

Data Analysis. The copolymer density profile is calculated by transforming the SLD profiles that are found to most accurately fit

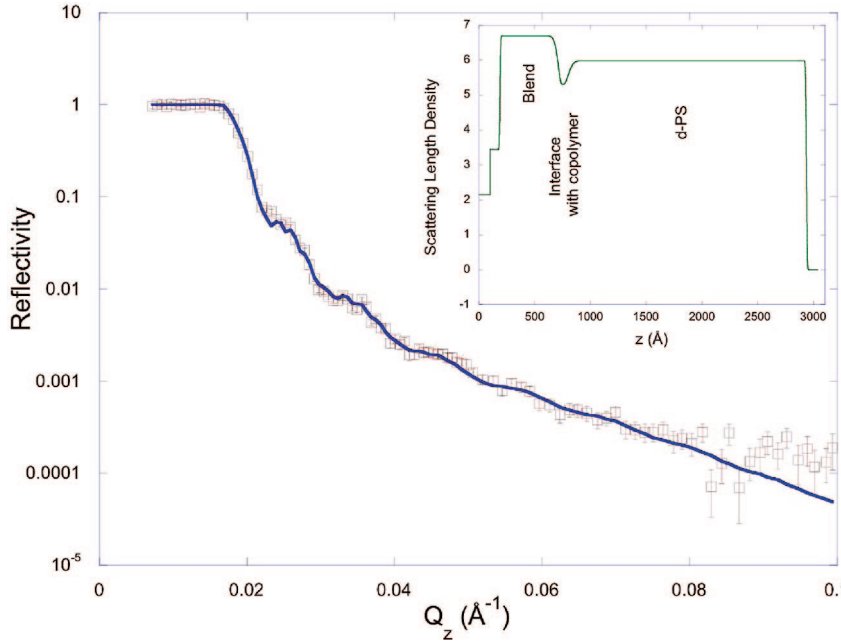

Figure 3. NR profile and fit to the ran54 bilayer sample annealed at 150 °C for 420 min. The circles are the measured points, and the solid line represents the calculated fit. The inset is the model SLD profile used to fit the reflectivity data.

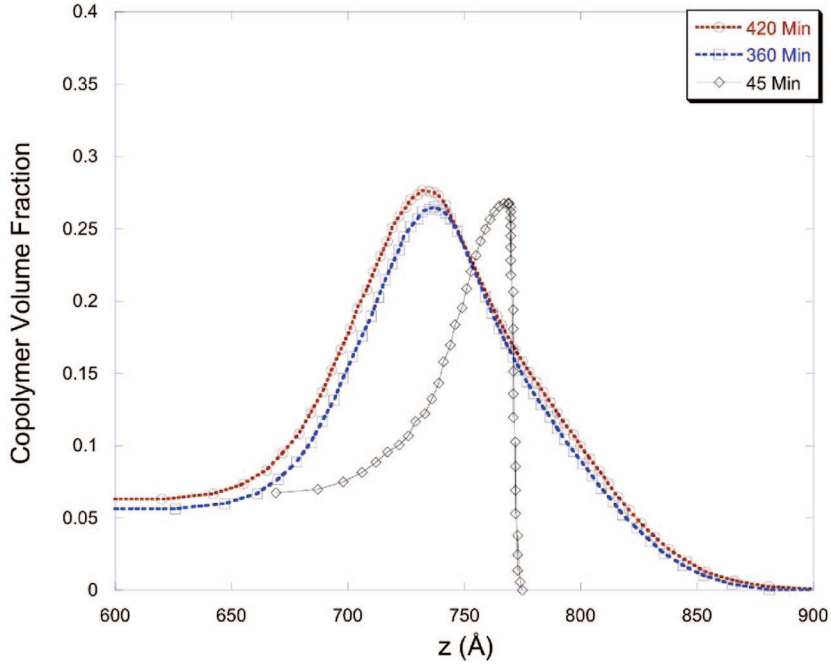

Figure 4. Evolution of the ran54 copolymer density profile at the d-PS/d-PMMA interface as a function of annealing time at 150 °C.

the reflectivity data of the samples to provide the copolymer volume fraction, Φ_z, density profile as a function of the depth, z:

$$\Phi_z = \{(\mathrm{SLD})_\mathrm{d} - (\mathrm{SLD})_{m(z)}\}/\{(\mathrm{SLD})_\mathrm{d} - (\mathrm{SLD})_\mathrm{c}\} \qquad (1)$$

where $(\mathrm{SLD})_\mathrm{d}$ is the scattering length density of the deuterated polymer, $(\mathrm{SLD})_{m(z)}$ is the scattering length density of the fitted profile at position z, and $(\mathrm{SLD})_\mathrm{c}$ is the scattering length density of the protonated copolymer (1.22×10^{-6} Å). Figure 4 shows the evolution of the copolymer volume fraction for the ran54 copolymer as a function of the depth, z, at different anneal times. The figure demonstrates that the breadth of the interfacial region as well as the amount of copolymer increases with increasing annealing time due to the segregation of the copolymer to the interface. To quantify the dynamics of the segregation of the copolymer to the interfacial region, we employ the model developed by Kramer and Jones which describes the kinetics of the growth of the surface excess layer, invoking a depletion layer that neighbors the surface excess layer. Using the copolymer density profile derived from neutron reflectivity, the copolymer interfacial excess, Z^*, is calculated as

$$Z^* = \int (\Phi_\mathrm{c}(z) - \Phi_\mathrm{b})\, \mathrm{d}z \qquad (2)$$

where $\Phi_\mathrm{c}(z)$ and Φ_b are the copolymer volume fraction at depth z and the copolymer volume fraction in the PMMA layer far from the interface, respectively. Thus, Φ_b is used as the baseline for the integration, whose limits are from a low value of z where $\Phi_\mathrm{c}(z) = \Phi_\mathrm{b}$ to the upper part of the copolymer density profile where $\Phi_\mathrm{c}(z)$ approaches zero, as can be observed in Figure 4. This time evolution of the interfacial excess was then analyzed to quantify the dynamics of the segregation of these random copolymers to the d-PS/

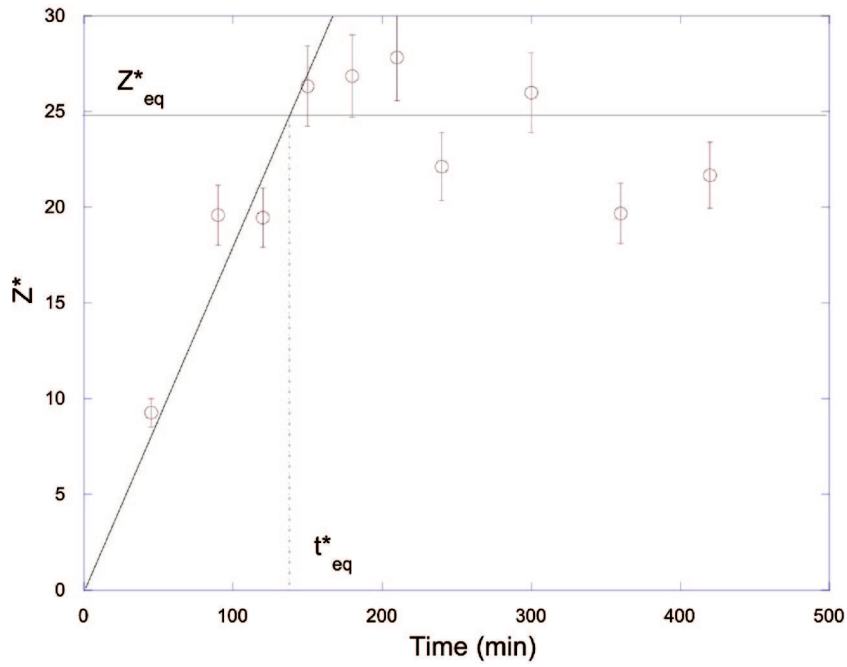

Figure 5. The interfacial excess, Z^*, for the Ran54 copolymer as a function of annealing time at 150 °C obtained from NR measurements.

Table 2. Neutron Reflectivity Results for the P(S-*ran*-MMA) Interfacial Segregation Process

Φ_{MMA}	Z_{eq} (cm)	t_{eq} (s)	D_m (cm^2/s)	D_A* (cm^2/s)	ζ_{eff} (dyne-s/cm)
0.5	5.0×10^{-7}	1.23×10^4	2.0×10^{-15}	2.2×10^{-15}	7.8×10^{-4}
0.54	2.77×10^{-7}	9.00×10^3	8.5×10^{-16}	1.2×10^{-15}	2.6×10^{-3}
0.67	4.75×10^{-7}	3.33×10^4	6.8×10^{-16}	3.8×10^{-16}	5.8×10^{-3}
0.8	3.10×10^{-7}	1.26×10^4	7.2×10^{-16}	8.7×10^{-16}	4.6×10^{-3}

d-PMMA interface as described in the following sections and described in detail in our previous paper.[18]

Results

Interfacial Segregation. Figure 5 is a plot of the interfacial excess, Z^*, as a function of annealing time at 150 °C for the Ran54 copolymer. The figure illustrates that the interfacial excess grows at the d-PS/d-PMMA interface with increasing annealing time. Eventually, the segregation processes cease and Z^* remains constant with further annealing. This leveling off period represents the saturation of the copolymer wetting layer at the interface and characterizes the equilibrium interfacial excess, Z^*, of the copolymer. In this case, a saturated wetting layer does not necessarily imply that the composition of the wetting layer is only one component, although a completely separate layer may form at the interface that consists of a single component. It indicates that further annealing does not increase the amount of the copolymer at the interface. This behavior was observed for all four copolymers that were studied. The time necessary for the segregation process to reach Z^* is the equilibrium time, t_{eq}, and is obtained by the intercept of a double extrapolation of the growth period and the leveling off period, as shown in Figure 5. For each sample, four estimates of t_{eq} determined from this plot are averaged to obtain the reported t_{eq}. In Table 2, t_{eq} is listed for each of the four copolymer blends that were examined. The standard deviation of this average value ranges from 3 to 7% and is taken as the percent error in Z_{eq} and t_{eq}.

Copolymer segregation to an interface occurs when the interfacial energy gain that results from the segregation is greater than the demixing energy loss associated with forming an enriched copolymer layer.[12,13] This indicates that the formation of the copolymer wetting layer at the interface reduces the interfacial tension between phases. Since our sample consists of a d-PMMA/copolymer blend layer that is capped with d-PS, there are repulsive forces between the d-PS and d-PMMA that are in contact at the as-cast interface between the two layers. Upon annealing, the S monomers in the copolymer are repelled from the d-PMMA and are attracted to the d-PS layer. As the annealing time increases, the amount of copolymer at the interface increases, indicating that the copolymer occupies a greater interfacial volume to minimize the repulsive forces that separate the interface.

Diffusion. Figure 6 shows a log–log plot of the interfacial excess growth as a function of annealing time for the Ran80 copolymer. The line through the data represents a power law fit to the portion of the curve where Z^* increases, illustrating the growth rate of the interfacial excess. The fit demonstrates that the interfacial excess growth scales as $t^{1/2}$, which is in agreement with the model of Kramer and Jones for the diffusion-limited growth of a polymer wetting layer at a surface or interface.[12,13] Similar scaling behavior was observed for all four copolymer systems. The growth of the wetting layer is controlled by the copolymer diffusion to the interface, where the copolymer diffuses to the d-PS/d-PMMA interface, while the d-PMMA simultaneously diffuses away from the interface. This phenomenon is referred to as mutual diffusion or interdiffusion. The depletion layer model of Kramer and Jones[12,13] predicts that the interfacial excess layer is saturated after a time which is related to the mutual diffusion coefficient of the segregating species by

$$D_m = (Z^*/\Phi_\infty)^2/t_{eq} \quad (3)$$

where D_m is the mutual diffusion coefficient of the copolymer, Z^* is the equilibrium interfacial excess, t_{eq} is the equilibrium time, and Φ_∞ is the equilibrium volume fraction of copolymer in the bulk homopolymer matrix. The mutual diffusion coefficients for all four copolymer compositions as determined using eq 3 are shown in Table 2. The magnitude of these mutual diffusion coefficients is in agreement with the mutual diffusion coefficients for alternating copolymers that have diffused to the d-PS/d-PMMA interface out of a d-PMMA matrix.[18]

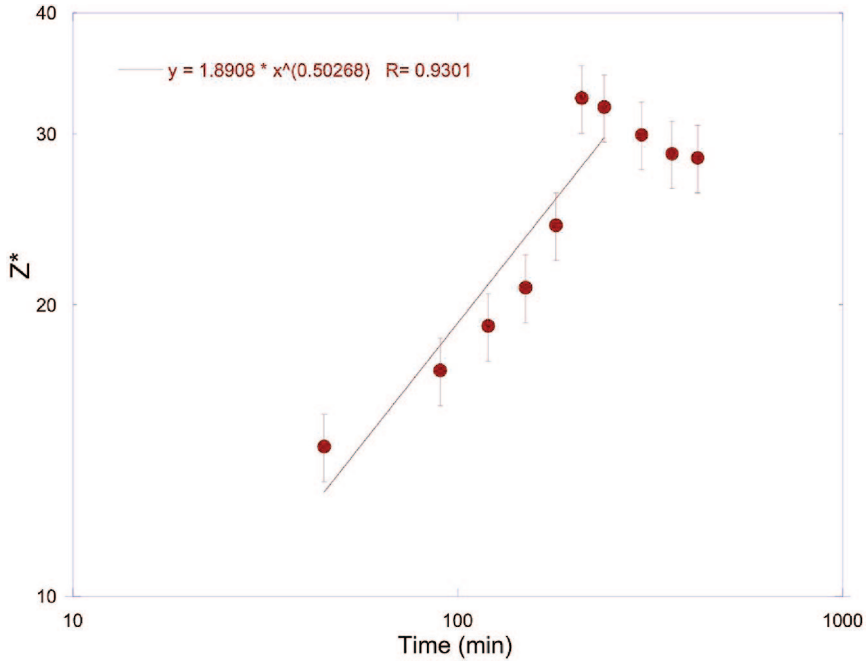

Figure 6. Log–log plot of the interfacial excess, Z^*, for the Ran80 copolymer as a function of annealing time at 150 °C obtained from NR measurements. The line represents a power law fit to the data.

D_m can then be correlated to the tracer diffusion coefficients of the two blend components using the fast mode theory of polymer interdiffusion[28]

$$D_A^* = [(D_m/2(\chi_s - \chi_{hc})/\Phi_A\Phi_B) - (\Phi_A D_B N_B)]/\Phi_B N_A \quad (4)$$

where D_A^* and D_B^*, N_A and N_B, and Φ_A and Φ_B are the tracer diffusion coefficients, degree of polymerization, and volume fractions of the copolymer and d-PMMA, respectively.[29] χ_s is the Flory–Huggins interaction parameter for the blend at the spinodal and χ_{hc} is the homopolymer/copolymer Flory–Huggins interaction parameter in the blend. Thus, the tracer diffusion coefficient for the segregating copolymer (component A) can be extracted from the measured D_m value if the tracer diffusion coefficients for the d-PMMA matrix component (polymer B) and the Flory–Huggins interaction parameters are known. D_B^* was estimated to be 2.01×10^{-19} cm^2/s for PMMA using a value of 0.39 dyn-s/cm for the friction factor of PMMA[18,23] and eq 7 below. The Flory–Huggins interaction parameter at the spinodal, χ_s, is estimated as

$$\chi_s = 1/2[(\Phi_A N_A)^{-1} + (\Phi_A N_B)^{-1}] \quad (5)$$

The homopolymer/copolymer χ, χ_{hc}, was estimated using the copolymer effect theory, which approximates χ_{hc} from the corresponding homopolymer/homopolymer χ parameter as[11,22]

$$\chi_{hc} = (\chi_{PS/PMMA})f^2 \quad (6)$$

where f is the monomer styrene composition of the copolymer and $\chi_{PS/PMMA}$ is the PS/PMMA χ parameter which is reported in the literature as 0.018[30,31] at $T = 423$ K. The tracer diffusion coefficients were then calculated for all four copolymer compositions using the experimentally determined mutual diffusion coefficients and eq 4 and are listed in Table 2. Our calculated values for the tracer diffusion coefficients are consistent with tracer diffusion coefficients for alternating copolymers.[18]

These calculated tracer diffusion coefficients can then be correlated to the effective friction coefficient, ζ_{eff}, using the reptation model of Doi and Edwards[32] which relates the tracer diffusion coefficient of a reptating polymer chain to its effective friction coefficient, ζ_{eff}, as

$$\zeta_{eff} = (k_b T d_t)/(3N^2 b^2 D_A^*) \quad (7)$$

where k_b is Boltzmann's constant, T is temperature in kelvins, $d_t = 7.3$ nm is the tube diameter for a PMMA molecule, $b = 0.87$ nm is the segment length of PMMA, and N is the degree of polymerization.[25] It should be noted that the values for b, d_t, and N will change for different systems. Using the calculated tracer diffusion coefficients and eq 7, the effective friction factors were calculated for all four copolymer compositions, and Figure 7 is a semilog plot of the effective friction factors, ζ_{eff}, as a function of the copolymer composition. Friction factors for PS and PMMA homopolymers as well as those for PS/PMMA disordered diblock copolymers in a PMMA matrix from ref 23 are also shown as a reference. The line is a guide to the eye and represents a linear-log average between the two homopolymer values. The figure demonstrates that while the friction factors for diblock copolymers at all compositions are essentially a linear-log average of the two homopolymer values, the friction factors for the random copolymers at the same compositions are up to an order of magnitude lower. This is consistent with our simulation results[7] which indicate that thermodynamic interactions between immiscible polymers have a strong impact on the dynamics and structure of random copolymers dispersed in a homopolymer matrix.

Discussion

Dynamics in multicomponent polymer systems are complicated by the fact that the presence of one component has a significant impact on the dynamics of the other. These effects are more dramatic for the PS/PMMA system, since PMMA has a friction factor that is 3 orders of magnitude higher than that of PS. Thus, the friction factors for the copolymers studied here should increase with increasing MMA content and our data indicate that, qualitatively, this is indeed the case. However, if the amount of MMA is the only factor that controls copolymer dynamics, friction factors for random copolymers should follow the same behavior as those observed for diblocks and lie on (or

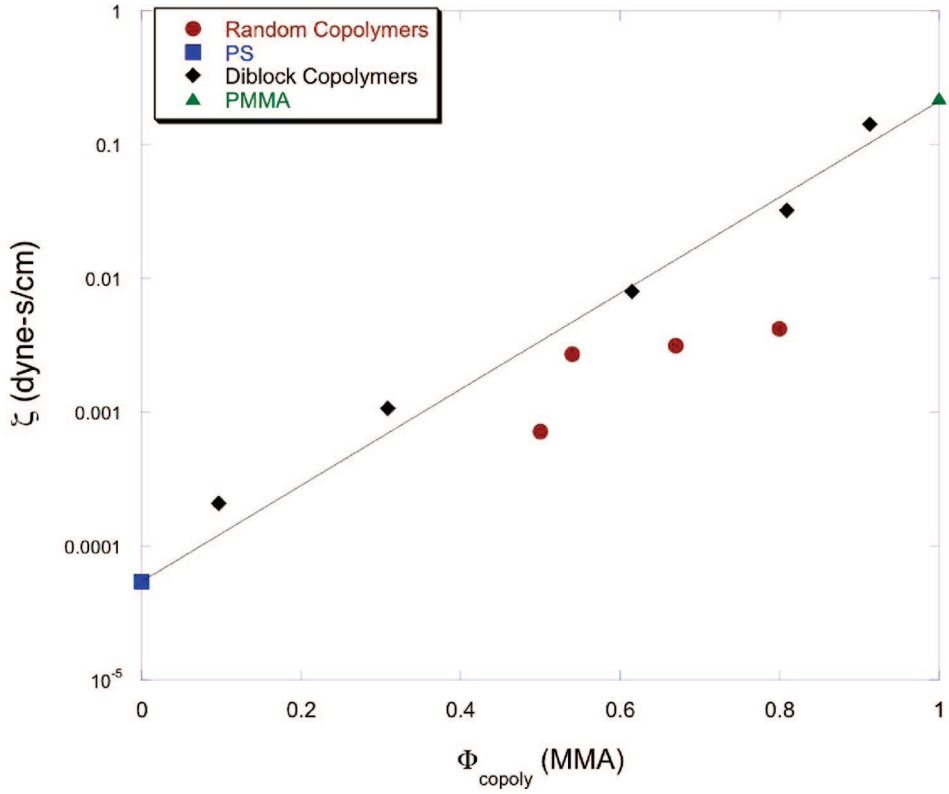

Figure 7. Semilog plot of the effective friction factor, ζ_{eff} as a function of the copolymer composition. Friction factors for PS and PMMA homopolymers as well as PS/PMMA diblock copolymers from ref 23 are also shown as a reference. The line is a guide to the eye. Error bars are within the symbol size.

near) the line shown in Figure 7. Our data clearly demonstrate that this is not the case for random copolymers and the dynamics of random copolymers are significantly faster than those of diblock copolymers with the same composition. Thus, factors other than the MMA content of the random copolymer play a significant role in determining their dynamics.

To gain further insights into this behavior, we have made an attempt to correlate our observations with predictions from the Lodge−McLeish[1] theory on the dynamics in multicomponent systems. This theory predicts that the local environment around any entity in a multicomponent system has a significant impact on its dynamics. This theory stipulates that, at the local level, the dynamic environment around a polymer in a blend is different from the average composition and, thus, the two blend components may experience different local environments even in a miscible blend. Thus, the theory predicts that the local dynamics around a monomer of type A in a multicomponent melt differ from that of the blend bulk composition due to chain connectivity. The effect of this change in dynamics with change in local composition is most obvious if the two blend components have distinctly different glass transition temperatures or friction factors. Moreover, the theory assumes that thermodynamic interactions between the two components of the blend have no impact on the local composition and uses purely geometric arguments based on chain connectivity to predict the effective composition around any monomer in a blend. In this theory, the effective local concentration, Φ_{eff}, around a monomer is given by

$$\Phi_{eff} = \Phi_s + (1 - \Phi_s)\Phi \tag{8}$$

where Φ_s is the self-concentration and Φ is the bulk composition for the two-component system. The self-concentration is calculated as

$$\Phi_s = C_\infty M_0/\kappa\rho N_{av} V \tag{9}$$

where C_∞ is the characteristic ratio, M_0 is the repeat unit molar mass, ρ is the density, κ is the number of backbone bonds per repeat unit, N_{av} is the average number of monomers per repeat unit and $V = l_k^3$ is the volume around a Kuhn segment of length l_k. We have calculated Φ_s and Φ_{eff} for a monomer on the copolymer chain in our system by assuming that the values for C_∞, M_0, ρ, κ, N_{av}, and l_k for the copolymer chains are a compositional average of the corresponding values for PS and PMMA that are reported in the literature.[1] Our calculated values for Φ_s^{copoly} and Φ_{eff}^{copoly} are shown in Table 3. Using Φ_{eff}^{copoly} and the stoichiometric composition of the copolymer, Φ, we can calculate the effective composition of styrene, $\Phi_{eff}^{S} = \Phi \times \Phi_{eff}^{copoly}$, around a copolymer monomer, and these values are also shown in Table 3.

Table 3. Effective Local Concentration of the Copolymer

Φ_{MMA}	Φ_s^{copoly}	Φ_{eff}^{copoly}	Φ_{eff}^{S}
0.5	0.2599	0.333	0.1669
0.54	0.2591	0.333	0.1532
0.67	0.2564	0.330	0.1091
0.8	0.2539	0.328	0.0657

Examination of these numbers shows immediately that this theory will not explain our experimental results. The local styrene composition around the copolymer is significantly smaller than the mol % styrene in the copolymer, and therefore, the effective friction factor of the copolymer will be dominated by the methyl methacrylate, which results in an effective friction factor that is above the line in Figure 7, whereas our experimental results are below. In order to observe dynamics that are below the line in Figure 7, the local concentration of styrene around the copolymer chain must be *richer* in styrene than the composition of the copolymer.

Interestingly, our recent simulation results indicate that a repulsive interaction between the monomers in a random copolymer can result in a local environment that is richer in the minor component (styrene in these experiments) than the copolymer composition. The Lodge−McLeish theory and subsequent calculations assume that the thermodynamic interac-

Table 4. Effective Local Concentration of Styrene from Experimental and Model Systems

Φ_{MMA}	Φ_{eff}^{S} (measured)	Φ_{eff}^{S} (model)	Φ_{eff}^{S} (measured) − Φ_{eff}^{S} (model)
0.5	0.70	0.05	0.65
0.54	0.535	0.046	0.49
0.67	0.425	0.03	0.39
0.8	0.45	0.02	0.43

tion between the styrene and MMA monomers do not impact the conformation or aggregation state of the copolymer, while our previous simulation results indicate that this is not a valid assumption. However, the Lodge−McLeish theory can be used to estimate the local concentration of styrene around a copolymer that is required to observe the local effective friction factors that are found in Table 2.

Using the Lodge−McLeish model to determine the local friction factor from the effective local styrene composition first calculates the effective glass transition temperature, T_g^{eff}, for the copolymer chains using the Fox equation[33]

$$\frac{1}{T_g^{eff}} = \frac{\Phi_{eff}^{S}}{T_g^{PS}} + \frac{(1-\Phi_{eff}^{S})}{T_g^{PMMA}} \tag{10}$$

where Φ_{eff}^{s} is the calculated effective styrene composition and T_g^{PS} and T_g^{PMMA} are the calorimetric glass transition temperatures of polystyrene and PMMA, respectively. Using the effective glass transition temperature, the theoretical friction factor for the copolymer at $T = 423$ K is calculated using the Williams−Landell−Ferry (WLF) equation[34]

$$\log \frac{\zeta(T)}{\zeta(T_g)} = \frac{-C_1(T - T_g^{eff})}{C_2 + (T - T_g^{eff})} \tag{11}$$

where C_1 and C_2 are WLF parameters that are specific to each polymer, T is the temperature in kelvins, T_g^{eff} is the effective glass transition temperature calculated from eq 10, and $\zeta(T)$ and $\zeta(T_g)$ are the friction factors at temperature T and the glass transition temperature, respectively. For these calculations, we have assumed that the WLF parameters as well as the friction factor at T_g, $\zeta(T_g)$, are a compositional average of those for homopolymer melts of polystyrene and PMMA, which are reported in the literature.[23]

Moreover, by following the same procedure in reverse order, the effective local composition around copolymer chains in our system can be estimated from the measured effective friction factor. This calculation yields an indication of the local effective composition that exists around a copolymer segment in the P(S-*ran*-MMA)/d-PMMA blend. Using the WLF equation, eq 11, and our measured effective friction factors at $T = 423$ K, the effective glass transition temperature, T_g^{eff}, is determined for each copolymer composition. As in the previous case, it is assumed that the WLF parameters C_1 and C_2 as well as the friction factor at the glass transition temperature, $\zeta(T_g)$, are compositional averages of the corresponding values for PS and PMMA that are obtained from the literature.[23] These calculated values of T_g^{eff} along with eq 10 were used to calculate the effective local composition, Φ^{eff}, and these calculated values are shown in Table 4. As mentioned qualitatively earlier, the data indicate that, for all four copolymers, the value of the effective composition as estimated from our experimental data is richer in styrene than the composition of the copolymer or the Lodge−McLeish prediction.

This is in agreement with our simulation results[7] on the dynamics of random copolymers in a homopolymer matrix, which demonstrate that the local composition around a copolymer chain is richer in the component that is not the same as the matrix chains. Analysis of the structure of the copolymers in the simulation studied indicate that the copolymer chains formed temporary aggregates or folded back on themselves (i.e., created a more compact conformation than an ideal chain) to minimize unlike contacts. This leads to a higher concentration of the minority species at the local level. Since the Lodge−McLeish model uses geometric arguments to predict the self-concentration and does not include thermodynamic effects, it consistently underestimates the increase in the concentration of styrene monomers in the local environment around a copolymer, which our simulation studies indicate are driven by repulsive interactions between the styrene and MMA monomers on the copolymer chains.

To further quantify the impact of the repulsive interaction on the local environment, the difference between the local styrene composition that is derived from the experimental results and the local styrene composition if the copolymer is homogeneously distributed in the d-PMMA matrix (copolymer loading in the blend * copolymer composition) is also listed in Table 4 and plotted as a function of copolymer composition in Figure 8. This figure qualitatively mimics the trends observed in our simulation, most clearly in Figures 11–13 of ref 7, which depict the conformation of the copolymer chain in the homopolymer matrix. These previous results show that as the percent A monomer (=MAA experimentally) in the copolymer increases from 50 to 66%, the size of the polymer chain increases due to fewer repulsive A−B interactions, and levels off above that. The radial distribution functions of the copolymers indicate that this change in copolymer expansion is a direct result of a decrease in the number of B−B (styrene−styrene) interactions among the polymer chain; i.e., the 50% copolymer chain is more contracted to form intramolecular B−B (styrene−styrene) interactions than the 66% MMA copolymer; thus, the local concentration of styrene around a given copolymer monomer exceeds that of the copolymer composition due to thermodynamic repulsion between the styrene and MMA monomers, as is observed in Figure 8. In the simulation, further increasing the % MMA in the copolymer beyond ca. 66% provides only slight changes in the conformation (and thus local environment) of the copolymer, which also agrees with the data in Figure 8.

Thus, Figure 8 demonstrates that the calculations using the Lodge−McLeish model consistently underestimate the self-concentration effect for nonathermal systems. Our results demonstrate that the repulsive interactions between styrene and MMA monomers on the copolymer chains lead to an increase in the local concentration of styrene monomers in the vicinity of a copolymer chain. This, in turn, has a significant impact on the dynamics of the copolymers as they diffuse through the PMMA matrix. These results are consistent with our simulations, which demonstrate that thermodynamic interactions play a significant role in determining the structure and dynamics of copolymers in a homopolymer matrix. When the two components of the copolymer have repulsive interactions, the system tries to minimize unlike contacts while maximizing like contacts. Depending on the copolymer composition, this is accomplished by the copolymer chains either folding back on themselves or forming temporary interchain aggregates. In both cases, the local copolymer composition is richer in the minority species. For our system, this implies that the effective composition around a copolymer is richer in styrene. However, the Lodge−McLeish model assumes that chain connectivity alone determines the local composition and does not include thermodynamic contributions. Hence, it follows that the model underestimates the self-concentration effect.

It is important to note that while these results demonstrate the impact of copolymer composition on its local environment, the calculations that we use to determine the effective composition are approximations based on the WLF parameters for pure

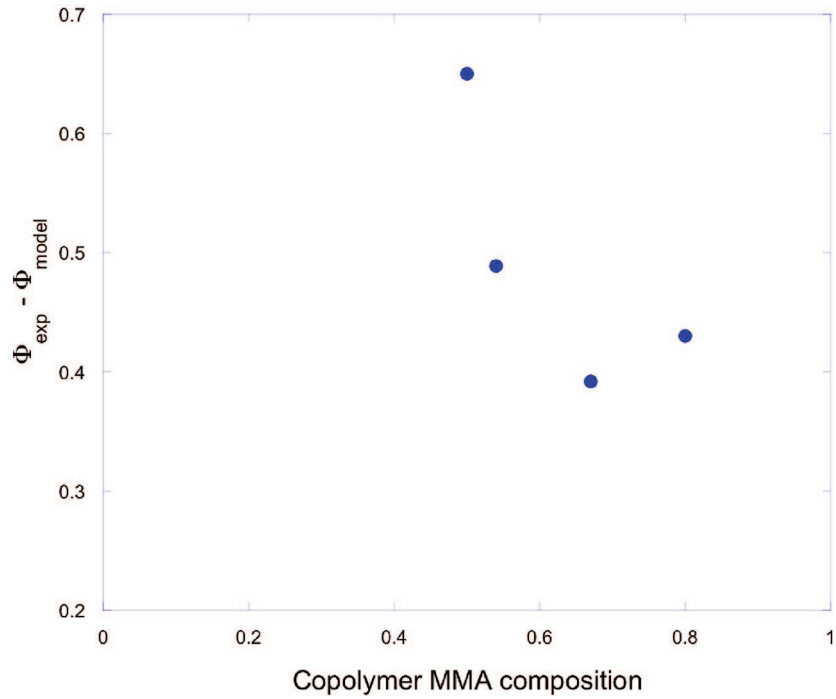

Figure 8. Plot of the difference between the measured effective styrene composition of the copolymer from the reflectivity experiment and the mole percent styrene in the copolymer blend. This plot provides a measure of the impact of the thermodynamic interaction between the MMA and styrene within the copolymer on the local environment of the copolymer, as detailed in the text.

PS and PMMA melts. We expect that knowledge of the WLF parameters for the specific copolymers will yield a more accurate measure of the effective composition. Hence, we are currently in the process of carrying out quasi-elastic neutron scattering (QENS) measurements on these systems at different temperatures in order to study the temperature dependence of the segmental relaxation times and extract WLF coefficients for each copolymer composition. Nonetheless, our results clearly show that even modest thermodynamic interactions between polymer chains significantly impact their dynamics and that the dynamics of a copolymer in a homopolymer matrix is an ideal model to examine the importance of thermodynamic interactions in the dynamics of multicomponent systems. Further experiments are underway in our laboratory to take advantage of this.

Conclusions

The effect of copolymer composition on the dynamics of the segregation process of P(S-*ran*-MMA) has been studied using neutron reflectivity. Our results indicate that copolymer composition has a significant impact on the dynamics of random copolymers. The monomeric friction factors increase with increasing MMA content in the copolymer. Since the friction factor of PMMA is 3 orders of magnitude higher than that of PS, the increase in friction factor for our copolymers could be attributed to the increasing MMA content. However, comparison between our measured friction factors with those for disordered diblock copolymers indicates that the friction factors for random copolymers are up to an order of magnitude lower than those for diblock copolymers at the same composition. This indicates that while the amount of MMA in the copolymer has an impact on dynamics, it is not the only factor that controls the dynamics in random copolymers. Analysis of the dynamic data using the Lodge−McLeish model indicates that the effective composition around a copolymer is richer in styrene than the predictions of the model based solely on chain-connectivity effects. Our data demonstrate that thermodynamic interactions between styrene and MMA monomers on the copolymer chains lead to an increase in the local concentration of styrene monomers around a copolymer chain, which leads to a decrease in the monomeric friction factor of the copolymers due to thermodynamic interactions. This is consistent with our simulation results and indicates that the styrene monomers in the copolymer may be aggregating in order to minimize contact with the matrix PMMA chains. Therefore, copolymer composition and thermodynamic interactions have a significant impact on their dynamics as well as structure as they diffuse through a homopolymer melt, and thus, a copolymer/homopolymer blend is an ideal system to examine the impact of thermodynamic interactions on dynamics in multicomponent polymer systems.

Acknowledgment. This research was sponsored by the Division of Material Sciences and Engineering, Office of Basic Energy Sciences, U.S. Department of Energy, under Contract No. DE-AC05-00OR22725, managed and operated by UT-Batelle, LLC. M.D.D. acknowledges financial support from the Centre National de la Recherche Scientifique and Université Louis Pasteur, and the authors would like to thank Jörg Baschnagel for helpful discussions during the course of this project. The authors also thank the Neutron Sciences Consortium at the University of Tennessee for funding of this project.

Supporting Information Available: An expanded discussion of the differences in Figures 2 and 3. This information is available free of charge via the Internet at http://pubs.acs.org.

References and Notes

(1) Lodge, T. P.; McLeish, T. C. B. *Macromolecules* **2000**, *33*, 5278.
(2) Kamath, S.; Colby, R. H.; Kumar, S. K.; Karatasos, K.; Floudas, G.; Fytas, G.; Roovers, J. E. L. *J. Chem. Phys.* **1999**, *111*, 6121–6128.
(3) Saxena, S.; Cizmeciyan, D.; Kornfield, J. A. *Solid State Nucl. Magn. Reson.* **1998**, *12*, 165–181.
(4) He, Y.; Lutz, T. R.; Ediger, M. D. *Macromolecules* **2003**, *36*, 8040–8048.
(5) He, Y.; Lutz, T. R.; Ediger, M. D.; Lodge, T. P. *Macromolecules* **2003**, *36*, 9170–9175.
(6) Kamath, S. Y.; Dadmun, M. D. *Macromol. Theory Simul.* **2005**, *14*, 519–527.

(7) Kamath, S. Y.; Dadmun, M. D. *J. Chem. Phys.* **2006**, *125*, 094902.
(8) Russell, T. P.; Brown, H. R.; Hawker, C. J.; Mayes, A. M.; Kulasekere, H.; Kaiser, H.; Ankner, J. F. *Macromolecules* **1996**, *29*, 5493.
(9) Bernard, B.; Brown, H. R.; Hawker, C. J.; Kellock, A. J.; Russell, T. P. *Macromolecules* **1999**, *32*, 6254.
(10) Winey, K. I.; Berba, M. L.; Galvin, M. E. *Macromolecules* **1996**, *29*, 2868.
(11) Sikka, M.; Pellegrini, N. N.; Schmitt, E. A.; Winey, K. I. *Macromolecules* **1997**, *30*, 445.
(12) Jones, R. A. L.; Kramer, E. J.; Ravailovich, M. H.; Sokolov, J.; Scharz, S. A. *Phys. Rev. Lett.* **1989**, *62*, 280.
(13) Jones, R. A. L.; Kramer, E. J. *Philos. Mag. B* **1990**, *62*, 129.
(14) Toral, R.; Chakrabarti, A.; Gunton, J. D. *Physica A* **1995**, *41*, 41.
(15) Nauman, B. E.; He, D. Q. *Chem. Eng. Sci.* **2001**, *56*, 1999.
(16) Puri, S.; Binder, K. *Phys. Rev. E* **1994**, *49*, 5359.
(17) Karim, A.; Mansour, A.; Felcher, G. P.; Russell, T. P. *Phys. Rev. B* **1990**, *42*, 6846.
(18) Arlen, M. J.; Dadmun, M. D.; Hamilton, W. A. *J. Polym. Sci., Part B* **2004**, *42*, 3235–3247.
(19) Balazs, A. C.; Demeuse, M. T. *Macromolecules* **1989**, *22*, 4260.
(20) Balazs, A. C.; Sanchez, I. C.; Epstein, I. R.; Karasz, F. E.; MacKnight, W. J. *Macromolecules* **1985**, *18*, 2188.
(21) Kulasekere, R.; Kaiser, H.; Ankner, J. F.; Russell, T. P.; Brown, H. R.; Hawker, C. J.; Mayes, A. M. *Physica B* **1996**, *221*, 306.
(22) Kulasekere, R.; Kaiser, H.; Ankner, J. F.; Russell, T. P.; Brown, H. R.; Hawker, C. J.; Mayes, A. M. *Macromolecules* **1996**, *29*, 5493.
(23) Milhaupt, J. M.; Lodge, T. P.; Smith, S. D.; Hamersky, M. W. *Macromolecules* **2001**, *34*, 5561.
(24) Bucknell, D. G.; Butler, S. A.; Higgins, J. S. *Macromolecules* **1999**, *32*, 5453.
(25) Achibat, T.; Boukenter, A.; Duval, E.; Lorentz, G.; Etienne, S. *J. Chem. Phys.* **1991**, *95*, 2949.
(26) Eastwood, E.; Dadmun, M. D. *Macromolecules* **2001**, *34*, 740.
(27) San Roman, A.; Madruga, E. L.; Del Puerto, M. A. *Macromol. Chem.* **1980**, *86*, 1.
(28) Kramer, E. J.; Green, P. F.; Palmstrom, C. J. *Polymer* **1984**, *25*, 473.
(29) Composto, R. J.; Kramer, E. J.; White, D. M. *Macromolecules* **1988**, *21*, 2580.
(30) Pellegrini, N. N.; Sikka, S. K.; Satija, S. K.; Iney, K. I. *Macromolecules* **1997**, *30*, 6640.
(31) de Gennes, P. G. *J. Chem. Phys.* **1980**, *72*, 4756.
(32) Doi, M.; Edwards, S. F. *The Theory of Polymer Dynamics*, 2nd ed.; Claredon Press: Oxford, U.K., 1988.
(33) Fox, T. G. *Bull. Am. Phys. Soc.* **1956**, *1*, 123.
(34) Ferry, J. D. *Viscoelastic Properties of Polymers*, 3rd ed.; Wiley: 1980.

MA0704212